Visualizing electron rearrangement in space and time during the transition from a molecule to atoms

Wen Li[a,b,1], Agnieszka A. Jaroń-Becker[a,1], Craig W. Hogle[a], Vandana Sharma[a], Xibin Zhou[a], Andreas Becker[a], Henry C. Kapteyn[a], and Margaret M. Murnane[a,1]

[a]JILA and Department of Physics, University of Colorado, Boulder, CO 80309; and [b]Department of Chemistry, Wayne State University, Detroit, MI 48202

Contributed by Margaret M. Murnane, October 7, 2010 (sent for review August 24, 2010)

Imaging and controlling reactions in molecules and materials at the level of electrons is a grand challenge in science, relevant to our understanding of charge transfer processes in chemistry, physics, and biology, as well as material dynamics. Direct access to the dynamic electron density as electrons are shared or transferred between atoms in a chemical bond would greatly improve our understanding of molecular bonding and structure. Using reaction microscope techniques, we show that we can capture how the entire valence shell electron density in a molecule rearranges, from molecular-like to atomic-like, as a bond breaks. An intense ultrashort laser pulse is used to ionize a bromine molecule at different times during dissociation, and we measure the total ionization signal and the angular distribution of the ionization yield. Using this technique, we can observe density changes over a surprisingly long time and distance, allowing us to see that the electrons do not localize onto the individual Br atoms until the fragments are far apart (~5.5 Å), in a region where the potential energy curves for the dissociation are nearly degenerate. Our observations agree well with calculations of the strong-field ionization rates of the bromine molecule.

electron dynamics | molecular dissociation | molecular dynamics

Probing the dynamic electron density distribution during a chemical reaction can provide important insights, making it possible to understand and control chemical reactions. For example, during the passage through a conical intersection, electronic excitation is rapidly converted into nuclear motion, and the nature of how the electron cloud rearranges is still poorly understood. Three distinct and promising approaches make it possible to probe electron dynamics in molecules. First, high harmonic generation from a molecule can exhibit characteristic features because of quantum interferences and diffraction of an electron originating from and then recolliding with the same molecule. Although the conditions under which accurate reconstruction of a complete electronic wave function is possible are still a topic of intense debate, nevertheless these characteristic interferences can reveal dynamical changes in the nuclear and orbital structure of a molecule as it changes configuration (1–4) or dissociates (5). In the case of dissociation, by measuring the amplitude and phase of the high harmonic signal from a dissociating molecule, destructive interferences in the high harmonic signal were observed that were attributed to recombination of a lone electron in a single excited state (5). To follow multielectron dynamics in a molecule, further work will be needed, because the quantum interference signal can be masked by competing contributions from different nearly degenerate valence orbitals, in particular at large internuclear distances.

A second recent approach for obtaining information about electron dynamics is to map the electron density distribution in the valence shells of a molecule, simply by measuring the molecular frame ionization yield after illumination by a strong laser field. Past work probing static molecules in the ground state has shown through both theory and experiment that the resulting ion yield reflects the symmetry of the molecular orbital from which the electron is ionized (6–11). As a result, strong-field ionization should be particularly attractive for capturing electron orbital dynamics because it directly relates to the electron density distribution (i.e., orbital shape) of a molecule.

In a third approach, the coupling between an excited electron and nuclear motion in a molecule can be probed by using time-resolved photoelectron spectroscopy (TRPES) (12–14). In TRPES, a vacuum ultraviolet (VUV) pulse is used to single-photon ionize a molecule, making this technique particularly useful for measuring how the binding energies of electrons in different valence orbitals change as the molecule dissociates. However, the linear response in a photoelectron spectroscopy measurement makes it challenging to follow shifts in the binding energies and to directly probe the varying electron density in the bond, on time and length scales for which the potential energy curves become nearly degenerate.

In this work, we use a femtosecond laser to strong-field ionize a molecule as it is undergoing photodissociation. In this experiment, the dissociation itself is initiated in a simple, single-photon transition by using a pump pulse. A higher intensity probe pulse is then used to ionize the molecule at various time delays, causing the fragments to fly apart rapidly with a distribution that reflects the instantaneous electron distribution. A cold target recoil ion momentum spectroscopy (COLTRIMS) reaction microscope then captures the dynamically changing angular distribution of the ionization fragments. Both the ionization rate and fragment angular distribution directly reflect how the entire valence shell electron density in a molecule rearranges, from molecular-like to atomic-like, as a bond breaks. These data can be successfully interpreted through careful comparison with theory. Our approach is unique to date, because of its ability to capture multielectron dynamics in a reaction up to significantly larger internuclear distances than can any other method. It also exhibits high sensitivity to small variations in the binding energy and electron density, as well as excellent time resolution compared with other approaches. This approach thus allows us to see that the electrons do not localize onto the individual Br atoms until the fragments are far apart (~5.5 Å), in a region where the potential energy curves for the dissociation are nearly degenerate.

Results

In our experiment, we use an ultrafast Ti:sapphire laser system in conjunction with a COLTRIMS apparatus (15). The sample consists of a neat bromine molecular beam entering the vacuum chamber through supersonic expansion. Dissociation of the Br_2 is initiated by a 400-nm ultrafast laser pulse (intensity

Author contributions: W.L., H.C.K., and M.M.M. designed research; W.L., A.A.J.-B., C.W.H., V.S., X.Z., and A.B. performed research; H.C.K. and M.M.M. contributed new reagents/analytic tools; W.L., A.A.J.-B., A.B., and H.C.K. analyzed data; and W.L., A.A.J.-B., A.B., H.C.K., and M.M.M. wrote the paper.

The authors declare no conflict of interest.

Freely available online through the PNAS open access option.

[1]To whom correspondence may be addressed. E-mail: wli@chem.wayne.edu, jaron@jilau1.colorado.edu, or Margaret.Murnane@colorado.edu.

This article contains supporting information online at www.pnas.org/lookup/suppl/doi:10.1073/pnas.1014723107/-/DCSupplemental.

PHYSICS

$\sim 2 \times 10^{11}$ W cm^{-2}, pulse duration $\sim$40 fs) generated by frequency doubling the 800-nm laser output. The absorption of a single 400-nm photon excites the bromine molecule from the ground state to the C ($^1\Pi_u$) dissociative state (Fig. S1). To confirm that the Br^+ ions are indeed originating from strong-field ionization of the dissociative C state, we measured the Br^+ yield as a function of pump beam power and found it to be linear (Fig. S2). An intense time-delayed 800-nm ($\sim 4 \times 10^{13}$ W cm^{-2}, $\sim$30 fs) laser pulse, with polarization orthogonal to the 400-nm pump, is used to ionize the dissociating bromine molecules to produce Br^+. We then detect the angular distribution of the resultant ions at different times during the dissociation (see Fig. 1 and Movie S1). Given that the dissociation is a prompt process, we therefore know how the electron density in the molecule changes as the molecule dissociates into two atoms. Fig. 2 plots the total ion yield as a function of time delay between the 400-nm dissociating pulse and the 800-nm probe pulse. The total ion yield initially increases for time delays up to 30 fs, at which point it decreases slightly, followed by an increase at time delays around 100 fs. As we will show below by comparing detailed theory and experiment, the first peak corresponds to ionization of electrons from π orbitals, whereas second peak can be explained by additional ionization channels opening up as different σ valence electrons are ionized. Finally, the ion yield drops quickly at time delays between ≈120 and 140 fs, limited by the time resolution in our experiment.

To interpret the experimental data, we calculated the ionization rate from the dissociative C state of Br_2 as a function of internuclear distance by using the molecular strong-field approximation (16) (see *Methods*). The results of these calculations can be plotted in terms of the final kinetic energy release (KER) of the fragments as a function of time delay. The calculated KERs shown in Fig. 3*B* are in very good agreement with our experimental measurements (Fig. 3*A*). We note that the characteristic features of the distributions are slightly shifted to longer time delays in the theoretical results, which may be attributed to the sensitive dependence of the conversion from distance to time delay on the specific form of the C-state potential energy curve (Fig. S1).

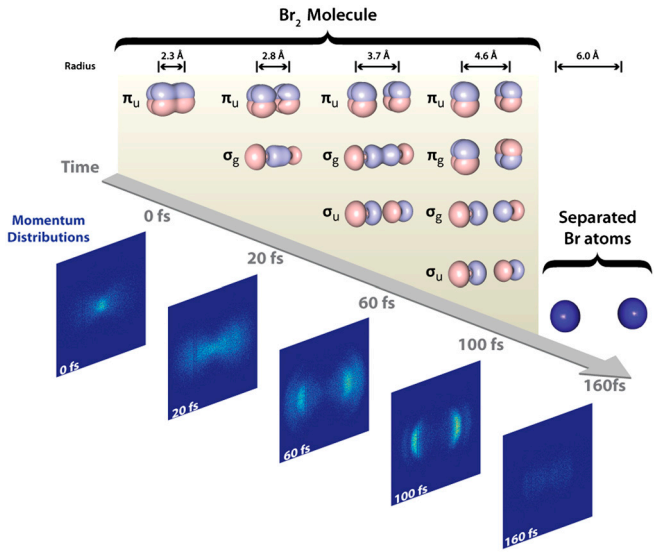

Fig. 1. (*Upper*) Calculated electron density (molecular orbitals) as a function of Br_2 internuclear separation and time after a 400-nm dissociating pulse causes the bond to rupture on the dissociative C neutral state. Note that contributions from all 10 electrons in the valence shells are included. (*Lower*) Measured angular dependence of the Br^+ ion yield from strong-field ionization of the Br_2 molecule, as a function of time after the dissociating pulse (see also Movie S1 for a movie of the data). Both experiment and theory indicate that the electrons localize onto individual atoms on a time scale ≈140 fs after the dissociating pulse.

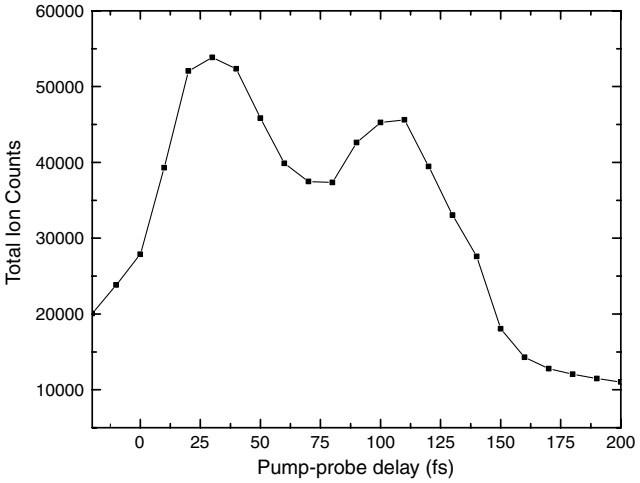

Fig. 2. Experimental Br^+ total ion yield as a function of time delay between the 400-nm dissociating pulse and the 800-nm probe ionizing pulse.

The calculations of Fig. 3 indicate that we are experimentally observing the entire valence shell of Br_2 (all ten electrons) evolving in time as the bond breaks, as shown in Fig. 1 *Upper*. The electron configurations of the ground X and dissociative C states of Br_2 are $[\text{core}](1\sigma_g)^2(1\sigma^*_u)^2(2\sigma_g)^2(1\pi_u)^4(1\pi^*_g)^4(2\sigma^*_u)^0$ and $[\text{core}](1\sigma_g)^2(1\sigma^*_u)^2(2\sigma_g)^2(1\pi_u)^4(1\pi^*_g)^3(2\sigma^*_u)^1$, respectively. Removal of one electron from different orbitals of the C state of Br_2 leads to different electronic configurations of the cation. For example, strong-field ionization of the singly occupied molecular orbital ($2\sigma^*_u$) electron primarily produces Br_2^+ in its ground state X with electronic configuration: $[\text{core}](1\sigma_g)^2(1\sigma^*_u)^2(2\sigma_g)^2(1\pi_u)^4(1\pi^*_g)^3(2\sigma^*_u)^0$. This state, as well as certain excited states of bound character, will not produce Br^+ at short internuclear distances during the dissociation process. At short time delays (below 20 fs), slow Br^+ ions are instead generated predominantly by ionizing the inner valence orbital $1\pi_u$. After dissociating for about 20 fs, the atoms have gained enough kinetic energy such that ionization from $2\sigma_g$ and $2\sigma^*_u$ opens additional channels for the dissociation of Br_2^+. The additional channels that continue to open up also explain why the total ionization yield increases as a function of time delay. At long time delays, fast Br^+ ions originate primarily from ionizing $2\sigma_g$, with minor contributions from other orbitals. The peak around 60 fs in Fig. 3 results from strong contributions of electron removal from $2\sigma_u$. Thus, we are able to identify the specific molecular orbitals that contribute primarily to the ionization and kinetic energy release signals up to a time delay of $\approx 140 \pm 15$ fs. This analysis indicates that the system still must be considered molecule-like and the electrons in the valence shell(s) of the system are still rearranging their configuration at these relatively long times (corresponding to internuclear separations of >5 Å). This finding is surprising because by then, according to our calculations, the four valence orbitals in the Br_2 molecule are nearly degenerate and the electron probability density at the midpoint between the two nuclei is 10 orders of magnitude smaller than the peak maximum.

Discussion

To physically interpret our findings, we plot the experimental angular distribution of Br^+ as a function of time delay for both the slow Br^+ (Fig. 4*A*, kinetic energy release below 0.7 eV) and fast Br^+ (Fig. 4*B*, kinetic energy release above 0.7 eV). We fit the angular distribution to a simple $\cos^n(\theta)$ [θ is the angle between the molecular axis and probe (ionizing) laser polarization]. Because photoexcitation of the C state is a perpendicular transition (17), the observed angular distributions of Br^+ are convolutions of the Br_2 excited state molecule axis alignment [$\cos^2(\theta)$ distribution] and the angular dependence of the Br_2 ionization rates.

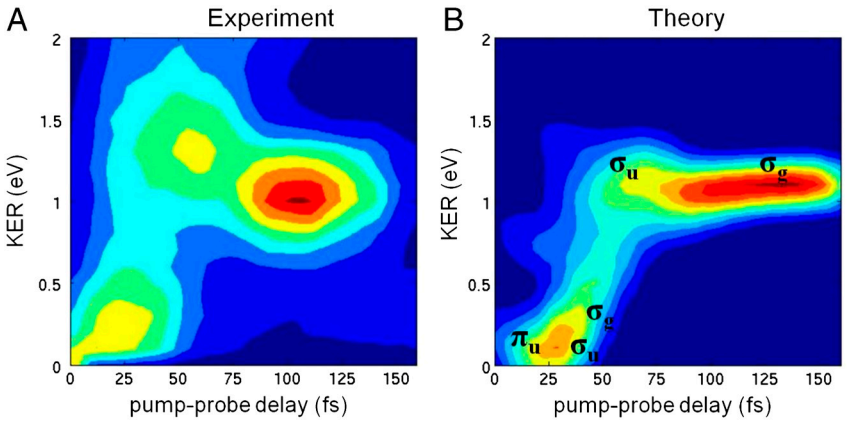

Fig. 3. Experimental (*A*) and calculated (*B*) total KER (i.e., recoil energy) of the Br^+ as a function of time after the dissociating pulse. At short time delays (below 20 fs), Br^+ ions are generated predominantly by ionizing the inner valence orbital $1\pi_u$ of the molecule. After dissociating for about 20 fs, the atoms have gained enough kinetic energy such that ionization from $2\sigma_g$ and $2\sigma^*_u$ opens additional channels for the dissociation of Br_2^+.

Thus, the sign of $n-2$ (plus or minus) shows whether the ionization is peaked parallel (+) or perpendicular (−) to the laser polarization, reflecting ionization from specific molecular orbitals. At short time delays, slow Br^+ has an n below 2, indicating ionization from the π_u state, whereas for fast Br^+, the ionization yield is highest along the molecular axis, indicating ionization predominantly from a σ-state. These findings are in agreement with our calculations (Figs. 1 and 3). More importantly, we observe such molecular-specific features up to time delays of 140 fs.

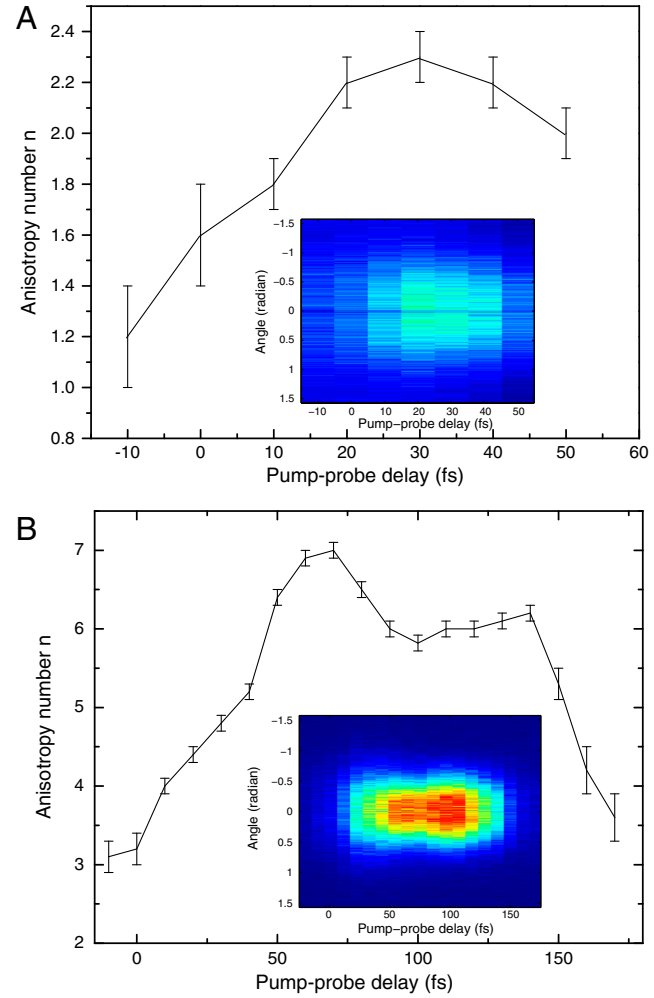

Fig. 4. Angular distribution of Br^+ at different time delays after the dissociating pulse, for both the slow Br^+ (*A*) (kinetic energy release below 0.7 eV) and fast Br^+ (*B*) (kinetic energy release above 0.7 eV). (See text for the fitting method for the anisotropy number *n*.)

After this time, the ion angular distributions flatten and appear to resemble ionization from separated atoms; i.e., the distribution reflects only the initial excited state molecule axis alignment in Br_2.

We also calculated the alignment dependence of the ionization rate, taking into account that in the experiment, the excited Br_2 are prepared with a $\cos^2(\theta)$ alignment of the molecular axis to the polarization direction. The results of our calculations are shown in Fig. S3. By comparing the changes in the experimental (Fig. 4) and calculated (Fig. S3) alignment dependence of the ionization rate, good qualitative agreement is apparent.

Finally, we believe that we are not inducing significant laser-field-driven electron dynamics, for several reasons. First, the most important point in discussing the possible role of strong-field effects is that, although our technique uses a relatively strong laser pulse as a *probe* of the molecular dynamics, our technique allows us to avoid strong-field effects in *initiating* the dynamics that we observe. Comparing our approach to TRPES, where the VUV probe pulse is capable of photoionizing even ground-state Br_2, in TRPES, a relatively intense pump pulse has to be used to obtain significant fractional population in the excited state. Thus, in TRPES, strong-field effects in the excitation step might explain the more rapid dissociation times observed in previous experiments (≈85 fs) (18). In our experiment, an ion signal emerges *only* from the dissociating molecules and is thus background-free. The fact that we see a precipitous drop in signal at long time and distance scales clearly shows that our signal discriminates against both the initial and the final state of dissociation, allowing us to observe the entire dissociation process that was initiated by a clearly perturbative, single-photon, excitation (as demonstrated in Fig. S2). Moreover, our calculations agree well with the data, even without including laser-induced modifications of the initial electronic state or charge-resonance-enhanced ionization (19, 20). Finally, the calculated kinetic energy releases and angular distributions do not change for a range of probe laser intensities ($4–5 \times 10^{13}$ W cm^{-2}) and for different ensembles of molecular orientations induced by the pump pulse (for further discussion, see *Ruling Out Laser-Field-Driven Effects* in *SI Text*).

In conclusion, we have demonstrated that we can image the electron density evolution of many electron states in the valence shell of a large diatomic molecular system up to time and distance scales at which the potential energy curves become nearly degenerate. We have shown that, because of the nonlinear interaction of an ultrashort intense laser pulse with the electrons, strong-field ionization can probe the electronic structure of a dissociating molecule even if the changes in the potential energy surfaces are small. Our studies show that both the ionization rate and the angular dependence of the ionization yield still vary strongly for internuclear distances at least 2 Å beyond where previous studies using photoelectron spectroscopy identified an establish-

ment of the atomic electronic structure in Br_2. We believe that the existence of such a molecular-like complex for large time and length scales is not restricted to Br_2 and should have broad implications for many fields such as photochemistry and reactive scattering dynamics. Interestingly, our observations and calculations are in good agreement with electron localization function calculations (21, 22), which indicate delocalization of the electrons in the different orbitals until internuclear separations >5.0 Å for Br_2 in the excited C state (Fig. S4). Thus, using strong-field ionization as a probe, we can follow electron dynamics in a bond over sufficiently long times to capture all the time scales during a chemical reaction.

Methods

In our calculations, the nonperturbative ionization rates for the transitions from the different orbitals into a field-dressed plane-wave state (or Volkov state) are determined. This method has been validated for obtaining total and alignment dependent ionization yields of di- and polyatomic molecules at equilibrium distances[7,16,23]. The potential energy curves of the C state Br_2 as well as of the ground and 29 excited contributing states in Br_2^+ (five for each of the possible symmetries: $^2\Sigma_g^+$, $^2\Sigma_g^-$, $^2\Sigma_u^+$, $^2\Sigma_u^-$, $^2\Pi_g$, and $^2\Pi_u$) as well as the corresponding wave functions are obtained by using aug-cc-pVQZ basis and multireference configuration interaction with relativistic and quadruple corrections (see Fig. S1 for details). The vertical ionization potentials for each possible ionization process and the respective kinetic energy release of the Br^+ were determined from the corresponding potential energy curves. The internuclear distance was converted to time delay by classical simulation of the dissociation along the potential energy curve of the C state, assuming that the pump pulse excites the molecule at $t = 0$ fs with an internuclear distance of $R = 2.3$ Å. The rates were convoluted by using Gaussians with standard deviations of 10 fs and 0.1 eV, respectively.

ACKNOWLEDGMENTS. We thank Army Research Office and Department of Energy for funding this project and thank the National Science Foundation Engineering Research Center for Extreme Ultraviolet Science and Technology for use of its facilities.

1. Li W, et al. (2008) Time-resolved dynamics in N_2O_4 probed using high harmonic generation. *Science* 322:1207–1211.
2. Zhou XB, et al. (2008) Molecular recollision interferometry in high harmonic generation. *Phys Rev Lett* 100:073902.
3. Itatani J, et al. (2004) Tomographic imaging of molecular orbitals. *Nature* 432:867–871.
4. Dudovich N, et al. (2006) Measuring and controlling the birth of attosecond XUV pulses. *Nat Phys* 2:781–786.
5. Worner HJ, Bertrand JB, Kartashov DV, Corkum PB, Villeneuve DM (2010) Following a chemical reaction using high-harmonic interferometry. *Nature* 466:604–607.
6. Jaron-Becker A, Becker A, Faisal FHM (2003) Dependence of strong-field photoelectron angular distributions on molecular orientation. *J Phys B: At, Mol Opt Phys* 36:L375–L380.
7. Jaron-Becker A, Becker A, Faisal FHM (2004) Ionization of N-2, O-2, and linear carbon clusters in a strong laser pulse. *Phys Rev A* 69:023410.
8. Lin CD, Tong XM (2006) Dependence of tunneling ionization and harmonic generation on the structure of molecules by short intense laser pulses. *J Photochem Photobiol, A* 182:213–219.
9. Pavicic D, Lee KF, Rayner DM, Corkum PB, Villeneuve DM (2007) Direct measurement of the angular dependence of ionization for N-2, O-2, and CO_2 in intense laser fields. *Phys Rev Lett* 98:243001.
10. Thomann I, et al. (2008) Direct measurement of the angular dependence of the single-photon ionization of aligned N-2 and CO_2. *J Phys Chem A* 112:9382–9386.
11. Tong XM, Zhao ZX, Lin CD (2002) Theory of molecular tunneling ionization. *Phys Rev A* 66:033402.
12. Bisgaard CZ, et al. (2009) Time-resolved molecular frame dynamics of fixed-in-space CS_2 molecules. *Science* 323:1464–1468.
13. Gessner O, et al. (2006) Femtosecond multidimensional imaging of a molecular dissociation. *Science* 311:219–222.
14. Sandhu AS, et al. (2008) Observing the creation of electronic Feshbach resonances in soft X-ray-induced O-2 dissociation. *Science* 322:1081–1085.
15. Gagnon E, et al. (2007) Soft X-ray-driven femtosecond molecular dynamics. *Science* 317:1374–1378.
16. Muth-Bohm J, Becker A, Faisal FHM (2000) Suppressed molecular ionization for a class of diatomics in intense femtosecond laser fields. *Phys Rev Lett* 85:2280–2283.
17. Cooper MJ, Wrede E, Orr-Ewing AJ, Ashfold MNR (1998) Ion imaging studies of the Br(P-2(J)) atomic products resulting from Br-2 photolysis in the wavelength range 260–580 nm. *J Chem Soc Faraday Trans* 94:2901–2907.
18. Wernet P, et al. (2009) Real-time evolution of the valence electronic structure in a dissociating molecule. *Phys Rev Lett* 103:013001.
19. Seideman T, Ivanov MY, Corkum PB (1995) Role of electron localization in intense-field molecular ionization. *Phys Rev Lett* 75:2819–2822.
20. Zuo T, Bandrauk AD (1995) Charge-resonance-enhanced ionization of diatomic molecular-ions by intense lasers. *Phys Rev A* 52:R2511–R2514.
21. Becke AD, Edgecombe KE (1990) A simple measure of electron localization in atomic and molecular systems. *J Chem Phys* 92:5397–5403.
22. Savin A, Silvi B, Colonna F (1996) Topological analysis of the electron localization function applied to delocalized bonds. *Can J Chem* 74:1088–1096.